Accurate Method for Calculating Mesopore Size Distributions from Argon Adsorption Data at 87 K Developed Using Model MCM-41 Materials

Michal Kruk and Mietek Jaroniec*

Department of Chemistry, Kent State University, Kent, Ohio 44242

Received August 30, 1999

Argon adsorption isotherms were measured at 87 K for two macroporous silicas and a series of high-quality MCM-41 silicas with approximately cylindrical pores of average diameters from 2 to 6.5 nm. The pore sizes of the MCM-41 samples were accurately determined in earlier studies on the basis of powder X-ray diffraction and nitrogen adsorption using a geometrical relation between the pore volume, pore−center distance, and pore size in the honeycomb structure. Thus acquired model argon adsorption data for cylindrical mesopores were used to determine the statistical film thickness in the pores and the relation between the pore core radius and the capillary condensation/evaporation pressure. The statistical film thickness curve (*t*-curve) was extrapolated over the entire pressure range by using data for suitable macroporous silicas. The *t*-curve is reported in forms of a simple empirical equation and tabulated data. The relation between the pore core radius and the capillary condensation pressure was interpolated and extrapolated over the range from about 2 to at least 50 nm using a suitable empirical equation, which is approximately equivalent to the Kelvin equation for large mesopore sizes. These relations were used in a standard procedure to calculate mesopore size distributions (PSDs). The obtained pore sizes were in excellent agreement with those evaluated on the basis of the geometrical method using X-ray diffraction (XRD) and primary mesopore volume data. Moreover, positions, heights, and widths of the PSD peaks in the primary mesopore range calculated from argon data were in remarkable agreement with those of the PSD data calculated from nitrogen adsorption data at 77 K using a properly calibrated method reported recently. The agreement extended also on the secondary mesopore range (above about 10 nm). The method also correctly reproduced MCM-41 total pore volumes obtained using a single-point method. Thus, an accurate and self-consistent method for calculating PSDs for silicas with cylindrical pores from argon adsorption data measured at 87 K was successfully developed. Moreover, the reported data for macroporous silicas can be used in comparative plot analysis to determine the external surface areas, primary mesopore volumes, and micropore volumes of microporous and mesoporous silicas.

Introduction

Gas adsorption is a well-established, popular, and highly informative method for characterization of porous structures of adsorbents and catalysts, allowing one to evaluate their specific surface areas and pore size distributions.[1,2] Nitrogen adsorption is now a standard technique for determination of the specific surface area and is a primary tool for evaluation of the pore size distributions.[1,2] Adsorption of other gases can also provide a valuable insight into properties of porous structures. For instance, argon at 87 K was found to be highly useful in studies of microporous materials, such as zeolites.[3,4] However, the potential of application of adsorptives other than nitrogen in characterization of porous solids is still far from being fully utilized, largely because of the insufficient knowledge of their adsorption behaviors, which manifests itself for instance in the lack of proper statistical film thickness data available in the literature.[1] To overcome this problem, one can calibrate the pore size analysis using some well-defined materials, but so far only crystalline microporous samples have been applied,[4] which are available in a very narrow range of pore sizes. The discovery of ordered mesoporous materials (OMMs)[5] opened new perspectives and created new challenges in the field of characterization of adsorbents using gas adsorption. These well-defined structures can be considered as model solids[6−12] to test both new and previously developed characterization

* To whom correspondence should be addressed. Telephone: (330) 672-3790. Fax: (330) 672-3816. E-mail: jaroniec@columbo.kent.edu.

(1) Gregg, S. J.; Sing, K. S. W. *Adsorption, Surface Area and Porosity*; Academic Press: London, 1982.
(2) Jaroniec, M.; Madey, R. *Physical Adsorption on Heterogeneous Solids*; Elsevier: Amsterdam, 1988.
(3) Saito, A.; Foley, H. C. *AIChE J.* **1991**, *37*, 429.
(4) Borghard, W. S.; Sheppard, E. W.; Schoennagel, H. J. *Rev. Sci. Instrum.* **1991**, *62*, 2801.
(5) Beck, J. S.; Vartuli, J. C.; Roth, W. J.; Leonowicz, M. E.; Kresge, C. T.; Schmitt, K. D.; Chu, C. T.-W.; Olson, D. H.; Sheppard, E. W.; McCullen, S. B.; Higgins, J. B.; Schlenker, J. L. *J. Am. Chem. Soc.* **1992**, *114*, 10834.
(6) Franke, O.; Schulz-Ekloff, G.; Rathousky, J.; Starek, J.; Zukal, A. *J. Chem. Soc., Chem. Commun.* **1993**, 724.

10.1021/cm9905601 CCC: $19.00
Published on Web 12/11/1999

methods and to either validate them for general or specific application or reveal their inapplicability.[9−12]

Argon adsorption was immediately recognized as a suitable tool for characterization of ordered mesoporous materials.[5,13−15] However, even after a calibration involving crystalline microporous materials,[4] analysis of argon adsorption data measured at 87 K provided inaccurate pore size values, and for instance, combined X-ray diffraction/argon adsorption data from ref 5 indicated an unrealistically small pore wall thickness of 0.3 nm for one of the samples studied. Argon adsorption in OMMs has also been the subject of numerous studies.[7,8,16−24] Most of them were aimed at improvement of the understanding of capillary condensation phenomena in uniform mesopores, and only the work of Neimark and co-workers[21−24] was focused mainly on improvement of pore size analysis using argon adsorption at 77 and 87 K. Their work led to development of methodology for calculation of pore size distributions by employing model isotherms calculated for ideal cylindrical pores by means of nonlocal density functional theory. However, this research effort still did not benefit fully from the discovery of OMMs, since it consisted of characterization of OMMs using advanced computational approaches rather than application of OMMs of well-known pore sizes to test and improve methods of adsorption characterization of porous solids.

A simple and effective approach for application of OMMs in the development of accurate tools for calculation of mesopore size distributions has recently been proposed by Kruk, Jaroniec, and Sayari (KJS).[12] The idea was to use adsorption data for OMMs with simple pore geometry and a wide range of available pore sizes accurately determined using independent methods (such as those reported in refs 11 and 25) to (i) find experimental relations between the capillary condensation/evaporation pressure and the pore size, (ii) calculate the statistical film thickness curves in pores, and (iii) identify relations, which are generally valid for all samples and thus potentially useful for the pore size analysis. Further, the approach involved (iv) extrapolation of these potentially useful relations over the entire range of pressures applied in the mesopore analysis using experimental data and/or proper generally known relations for large pores, (v) application of these extended relations to calculate mesopore size distributions using well-known methods, and finally (vi) examination of the accuracy of the pore size determination and the self-consistency of the approach. So far, the KJS approach was successfully applied to develop methodology of accurate and self-consistent determination of pore size distributions, pore volumes, and specific surface areas from nitrogen adsorption data measured at 77 K for porous silicas[12] as well as for hydrophobic materials[26] (such as organosilane-modified silicas) with cylindrical pores. In the current study, the KJS approach was used to test applicability of argon adsorption at 87 K for the mesopore size analysis and to derive relations suitable for accurate and self-consistent calculation of pore size distributions. The pore size distributions determined from argon adsorption data were critically compared with results of independent methods of pore size analysis, including the geometrical method[11,25] and the KJS-calibrated procedure employing nitrogen adsorption data at 77 K.

Table 1. Characteristics of the MCM-41 Samples under Study Based on Argon Adsorption Isotherms Measured at 87 K[a]

sample	source	S_{BET} ($m^2\ g^{-1}$)	V_t ($cm^3\ g^{-1}$)	p_{cc}/p_0	p_{ce}/p_0
(6.5)	27 [TR2d]	600	1.00	0.655	0.560
(6.0)	12 [(6.0)][b]	700	1.08	0.620	0.530
(5.5)	27 [TR3-24h]	680	0.97	0.595	0.500
(5.1)	28 [16C]	570	0.79	0.550	0.460
(4.6)	28 [16B]	460	0.61	0.500	0.435
(4.2)	28 [18]	690	0.90	0.440	0.415
(3.9)	28 [16A]	700	0.82	0.395	0.380
(3.6)	29 [BTR]	890	1.03	0.330	0.330
(3.1)	28 [12]	660	0.59	0.260	0.260
(2.8)	11 [C10][c]	850	0.65	0.200	0.200
(2.0)	11 [C8][c]	460	0.40	0.12[d]	0.12[d]

[a] Source; number of the reference where the synthesis and properties of the samples were reported (original notation is provided in brackets); S_{BET}, BET specific surface area; V_t, total pore volume; p_{cc}/p_0, relative pressure at the midpoint of the capillary condensation step; p_{ce}/p_0, relative pressure at the midpoint of the capillary evaporation step. [b] Synthesis described in ref 27. [c] These samples were prepared as described in ref 11, but calcined separately from those described therein. Thus, they have slightly different structural properties from the materials characterized in ref 11. [d] Broad and poorly pronounced steps of capillary condensation and capillary evaporation; some evidence of low-pressure hysteresis.

Experimental Section

Materials. MCM-41 samples used in the current study are listed in Table 1 along with references[11,12,27−29] to the descrip-

(7) Branton, P. J.; Hall, P. G.; Sing, K. S. W.; Reichert, H.; Schuth, F.; Unger, K. K. *J. Chem. Soc., Faraday Trans.* **1994**, *90*, 2965.
(8) Llewellyn, P. L.; Grillet, Y.; Schuth, F.; Reichter, H.; Unger, K. K. *Microporous Mater.* **1994**, *3*, 345.
(9) Ravikovitch, P. I.; Domhnaill, S. C. O.; Neimark, A. V.; Schüth, F., Unger, K. K., *Langmuir* **1995**, *11*, 4765.
(10) Naono, H.; Hakuman, M.; Shiono, T. *J. Colloid Interface Sci.* **1997**, *186*, 360.
(11) Kruk, M.; Jaroniec, M.; Sayari, A. *J. Phys. Chem. B* **1997**, *101*, 583.
(12) Kruk, M.; Jaroniec, M.; Sayari A. *Langmuir* **1997**, *13*, 6267.
(13) Vartuli, J. C.; Schmitt, K. D.; Kresge, C. T.; Roth, W. J.; Leonowicz, M. E.; McCullen, S. B.; Hellring, S. D.; Beck, J. S.; Schlenker, J. L.; Olson, D. H.; Sheppard, E. W. *Chem. Mater.* **1994**, *6*, 2317.
(14) Corma, A.; Kan, Q.; Navarro, M. T.; Perez-Pariente, J.; Rey, F. *Chem. Mater.* **1997**, *9*, 2123.
(15) Ryoo, R.; Ko, C. H.; Cho, S. J.; Kim, J. M. *J. Phys. Chem. B* **1997**, *101*, 10610.
(16) Llewellyn, P. L.; Grillet, Y.; Rouquerol, J.; Martin, C.; Coulomb, J.-P. *Surf. Sci.* **1996**, *352−354*, 468.
(17) Morishige, K.; Fujii, H.; Uga, M.; Kinukawa, D. *Langmuir* **1997**, *13*, 3494.
(18) Morishige, K.; Shikimi, M. *J. Chem. Phys.* **1998**, *108*, 7821.
(19) Sonwane, C. G.; Bhatia, S. K.; Calos, N. *Ind. Eng. Chem. Res.* **1998**, *37*, 2271.
(20) Storck, S.; Bretinger, H.; Maier, W. F. *Appl. Catal., A* **1998**, *174*, 137.
(21) Ravikovitch, P. I.; Wei, D.; Chueh, W. T.; Haller G. L.; Neimark, A. V. *J. Phys. Chem. B* **1997**, *101*, 3671.
(22) Ravikovitch, P. I.; Haller G. L.; Neimark, A. V. *Adv. Colloid Interface Sci.* **1998**, *76−77*, 203.
(23) Neimark, A. V.; Ravikovitch, P. I.; Grun, M.; Schuth, F.; Unger, K. K. *J. Colloid Interface Sci.* **1998**, *207*, 159.
(24) Ravikovitch, P. I.; Haller G. L.; Neimark, A. V. In *Fundamentals of Adsorption 6*; Meunier, F., Ed.; Elsevier: Paris, 1998; p 545.
(25) Dabadie, T.; Ayral, A.; Guizard, C.; Cot, L.; Lacan, P. *J. Mater. Chem.* **1996**, *6*, 1789.
(26) Kruk, M.; Antochshuk, V.; Jaroniec, M.; Sayari, A. *J. Phys. Chem. B* **1999**, *103*, 10670.
(27) Sayari, A.; Liu, P.; Kruk, M.; Jaroniec, M. *Chem. Mater.* **1997**, *9*, 2499.
(28) Kruk, M.; Jaroniec, M.; Kim, J. M.; Ryoo, R. *Langmuir* **1999**, *15*, 5279.
(29) Kruk, M.; Jaroniec, M.; Sayari, A. *Microporous Mesoporous Mater.* **1999**, *27*, 217.

Table 2. Reduced Adsorption Isotherm of Argon at 87 K on LiChrospher Si-1000 Silica[a]

p/p_0	α_s	p/p_0	α_s	p/p_0	α_s	p/p_0	α_s
1.29×10^{-5}	0.0026	2.837×10^{-3}	0.1153	0.03512	0.3604	0.540	1.197
1.54×10^{-5}	0.0049	3.116×10^{-3}	0.1206	0.0401	0.3804	0.560	1.228
2.41×10^{-5}	0.0071	3.401×10^{-3}	0.1258	0.0451	0.3993	0.580	1.261
3.48×10^{-5}	0.0093	3.692×10^{-3}	0.1309	0.0501	0.417	0.600	1.294
4.72×10^{-5}	0.0114	3.990×10^{-3}	0.1358	0.0590	0.445	0.620	1.329
6.10×10^{-5}	0.0134	4.29×10^{-3}	0.1407	0.0700	0.477	0.640	1.365
7.61×10^{-5}	0.0154	4.60×10^{-3}	0.1454	0.0800	0.503	0.660	1.403
9.23×10^{-5}	0.0174	4.92×10^{-3}	0.1500	0.0900	0.528	0.680	1.441
1.094×10^{-4}	0.0193	5.24×10^{-3}	0.1545	0.1000	0.550	0.700	1.483
1.276×10^{-4}	0.0211	5.62×10^{-3}	0.1597	0.1197	0.592	0.720	1.527
1.463×10^{-4}	0.0229	6.02×10^{-3}	0.1648	0.1397	0.631	0.740	1.575
2.059×10^{-4}	0.0281	6.42×10^{-3}	0.1698	0.1596	0.665	0.760	1.627
2.698×10^{-4}	0.0330	6.83×10^{-3}	0.1747	0.1797	0.697	0.780	1.682
3.390×10^{-4}	0.0377	7.52×10^{-3}	0.1830	0.2000	0.730	0.800	1.742
4.12×10^{-4}	0.0422	7.81×10^{-3}	0.1860	0.2202	0.759	0.820	1.806
4.89×10^{-4}	0.0464	8.06×10^{-3}	0.1888	0.2403	0.787	0.840	1.877
5.68×10^{-4}	0.0504	8.32×10^{-3}	0.1914	0.2604	0.815	0.859	1.957
6.48×10^{-4}	0.0541	8.57×10^{-3}	0.1941	0.2804	0.842	0.879	2.050
7.30×10^{-4}	0.0577	8.82×10^{-3}	0.1966	0.3005	0.869	0.899	2.154
8.11×10^{-4}	0.0610	9.08×10^{-3}	0.1991	0.3206	0.896	0.909	2.217
8.93×10^{-4}	0.0642	9.48×10^{-3}	0.2036	0.3407	0.923	0.919	2.285
9.76×10^{-4}	0.0672	9.80×10^{-3}	0.2065	0.3601	0.948	0.929	2.357
1.058×10^{-3}	0.0701	0.01008	0.2091	0.3800	0.974	0.938	2.438
1.138×10^{-3}	0.0728	0.01109	0.2185	0.400	1.000	0.948	2.535
1.349×10^{-3}	0.0795	0.01259	0.2315	0.420	1.027	0.960	2.67
1.572×10^{-3}	0.0860	0.01508	0.2509	0.440	1.054	0.969	2.81
1.805×10^{-3}	0.0923	0.01759	0.2685	0.460	1.081	0.981[b]	3.31
2.049×10^{-3}	0.0983	0.02008	0.2843	0.480	1.109	0.990[b]	3.72
2.303×10^{-3}	0.1042	0.02502	0.3123	0.500	1.137	0.993[b]	4.16
2.566×10^{-3}	0.1098	0.03006	0.3377	0.520	1.167		

[a] p/p_0, relative pressure; α_s, standard reduced adsorption (the amounts adsorbed for LiChrospher Si-1000 silica can be obtained by multiplying the α_s data by 7.813 cm^3 (STP) g^{-1}; the statistical film thickness curve for BJH calculations can be obtained by multiplying the α_s data by 0.5568 nm). [b] Data for LiChrospher Si-4000 silica (the corresponding amounts adsorbed can be evaluated by multiplying the α_s data by 3.244 cm^3 (STP) g^{-1}).

tion of their synthesis and properties. The samples are denoted as (*x*) MCM-41, where *x* stands for the pore diameter (rounded to the nearest 0.1 nm) determined from XRD/pore volume data as described below. Macroporous silicas LiChrospher Si-1000 and LiChrospher Si-4000 were acquired from EM Separations, Gibbstown, NJ.

Measurements. Argon adsorption isotherms were measured at 87 K using an ASAP 2010 volumetric adsorption analyzer manufactured by Micromeritics (Norcross, GA). Before the measurements, the samples were outgassed for about 2 h at 473 K in the degas port of the adsorption analyzer.

Calculation Methods. The BET specific surface area, S_{BET},[1] was evaluated from the data in the relative pressure range from 0.04 to 0.2, except for the samples with smaller pore sizes, for which adsorption data at lower relative pressures (0.04−0.1 for (3.1) and (2.8) MCM-41 and 0.02−0.06 for (2.0) MCM-41) were used to reduce overestimation of S_{BET} resulting from effects of capillary condensation in primary mesopores on the data in the BET range. It should be noted here that, in the current study, the IUPAC classification of pore sizes[30] is adopted, and accordingly, pores of the width below 2 nm, between 2 and 50 nm, and above 50 nm, are referred to as micropores, mesopores, and macropores, respectively. In studies of OMMs, it is helpful to further classify pores as primary mesopores (that is, ordered mesopores) and secondary mesopores (that is, other mesopores, and macropores up the width of about 200−400 nm, which are narrow enough for the capillary condensation to take place in the pressure range attainable by the adsorption equipment). The cross-sectional area used in the BET calculations for argon atom on the silica surface was equal to 0.138 nm^2.[1,7] The total pore volume, V_t, was evaluated from the amount adsorbed at a relative pressure of about 0.99[1,30] using the liquid argon density of 1.400 g cm^{-3} (evaluated using data from ref 1, p 166). The latter density was also used in other pore volume calculations performed. The external surface area, S_{ex}, and the primary mesopore volume, V_p, were evaluated using the α_s plot method[1] as described in detail elsewhere.[27] The standard reduced adsorption, α_s, is defined as a ratio of the amount adsorbed at a given relative pressure to the amount adsorbed at a relative pressure of 0.4. The α_s range used in calculations was chosen depending on the size of the primary mesopores and the presence or absence of secondary mesopores. Accordingly, the α_s range from 1.4 to 2.0 was used for (2.0), (3.6), (3.9), and (4.2) MCM-41 samples, the range from 1.8 to 2.4 was used for (2.8), (4.6), (5.1), (5.5), (6.0), and (6.5) MCM-41 samples, and the range from 1.6 to 2.0 was used for (3.1) MCM-41. The reference adsorption data used in the α_s plot analysis (Table 2) were based primarily on an argon adsorption isotherm measured at 87 K for LiChrospher Si-1000 silica with the argon BET specific surface area (calculated in the relative pressure interval from 0.04 to 0.2) equal to 19.3 m^2 g^{-1}. Since this adsorption isotherm exhibited capillary condensation at relative pressures above 0.97, α_s data for a macroporous silica with lower specific surface area (LiChrospher Si-4000; argon specific surface area = 8.1 m^2 g^{-1}) were used at pressures close to the saturation vapor pressure.

The primary mesopore diameter, w_d, for the samples under study was determined earlier[11,12,27−29] from the X-ray diffraction (XRD) and nitrogen adsorption pore volume data using the equation based on geometrical considerations of the ordered honeycomb structure characteristic of MCM-41:[11,25]

$$w_d = cd\left(\frac{\rho V_p}{1 + \rho V_p}\right)^{1/2} \quad (1)$$

where d_{100} is the XRD (100) interplanar spacing, c is a constant characteristic of the pore geometry, and ρ is the pore wall density (assumed to be 2.2 cm^3/g for silicas with amorphous pore walls).[11,19,25] The constant $c = 1.213$ for circular as well as hexagonal pores, but, in the latter case, the pore diameter,

(30) Sing, K. S. W.; Everett, D. H.; Haul, R. A. W.; Moscou, L.; Pierotti, R. A.; Rouquerol, J.; Siemieniewska, T. *Pure Appl. Chem.* **1985**, *57*, 603.

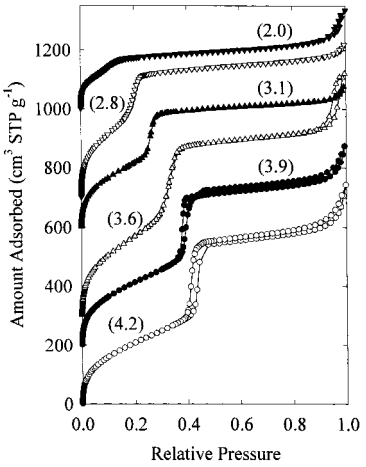

Figure 1. Argon adsorption isotherms measured at 87 K for MCM-41 samples with pore sizes below 4.5 nm.

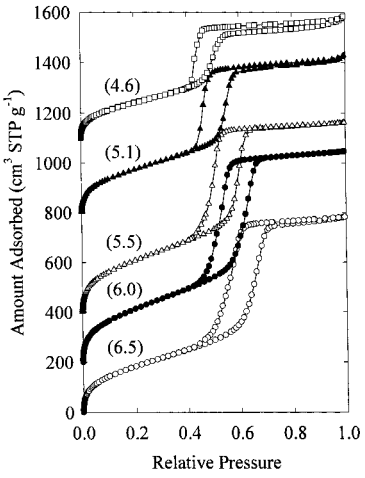

Figure 2. Argon adsorption isotherms measured at 87 K for MCM-41 samples with pore sizes above 4.5 nm.

w_d, is defined as the diameter of a circle of the same area as the hexagonal pore cross-section.[31] In the current study, MCM-41 pores were assumed to be cylindrical, unless noted otherwise. Although the primary mesopore volume used in the calculations based on eq 1 was evaluated from nitrogen adsorption data, the use of V_p calculated from data for other adsorptives, such as argon at 87 K, was reported to afford highly similar w_d values.[19] This can be attributed to the fact that differences in V_p values evaluated using different adsorptives are very small[19] and the results obtained using eq 1 are insensitive to such small differences in V_p, as discussed elsewhere.[31]

The statistical film thickness, $t(p/p_0)$, of argon adsorbate in MCM-41 pores (expressed as a function of the relative pressure, p/p_0) was calculated as follows:[12]

$$t(p/p_o) = \frac{w_d}{2}\left[1 - \left(\frac{\nu_{p,max} - \nu_p(p/p_0)}{\nu_{p,max}}\right)^{1/2}\right] \qquad (2)$$

where p is the equilibrium vapor pressure, p_0 is the saturation vapor pressure, and $\nu_{p,max}$ is the maximum amount adsorbed in primary mesopores. $\nu_p(p/p_0)$ is the amount adsorbed in the primary mesopores of MCM-41 as a function of the relative pressure determined as follows:[12]

$$\nu_p(p/p_0) = \nu(p/p_0) - \frac{S_{ex}}{S_{BET,ref}}\nu_{ref}(p/p_0) \qquad (3)$$

where $\nu(p/p_0)$ and $\nu_{ref}(p/p_0)$ are adsorption isotherms for the MCM-41 sample and the reference macroporous silica, respectively, S_{ex} is the external surface area of MCM-41, and $S_{BET,ref}$ is the BET specific surface area of the reference silica evaluated from argon adsorption data at 87 K. The adsorption capacity of primary mesopores of MCM-41 was assumed to be equal to the amount adsorbed at a relative pressure of 0.85: $\nu_{p,max} = \nu_p(0.85)$.

Results and Discussion

Argon Adsorption Isotherms at 87 K. Argon adsorption isotherms for the MCM-41 samples under study are shown in Figures 1 and 2. It can be seen that the position of the capillary condensation step gradually shifts to higher relative pressures and the relative height of the capillary condensation step increases with increasing pore diameter, which is analogous to the nitrogen adsorption at 77 K on MCM-41.[11,12,28,32] When the capillary condensation took place at relative pressures above about 0.35, adsorption−desorption hysteresis was observed. Hysteresis loops located close to this limiting pressure were usually triangular, since desorption branches were much steeper than adsorption branches[12] (see data for (3.9) and (4.6) MCM-41). The samples with yet larger pores exhibited hysteresis loops with parallel branches. This behavior closely follows the behavior of nitrogen at 77 K in MCM-41 pores.[12] As already observed in the latter case,[27,32] the shape of the hysteresis loop was found to be dependent on the sample quality, since the more highly ordered (4.2) MCM-41 exhibited the hysteresis loop with approximately parallel branches, whereas somewhat less ordered (4.6) MCM-41 exhibited a triangular hysteresis loop despite its larger pore size. It is also interesting to note that (5.1) and (4.2) MCM-41 had triangular hysteresis loops at their nitrogen adsorption isotherms at 77 K, but in the case of argon adsorption at 87 K, the isotherms had hysteresis loops with two parallel branches. Furthermore, (3.9) MCM-41 exhibited nitrogen adsorption isotherm with no hysteresis, whereas its argon adsorption isotherm at 87 K had a triangular hysteresis loop with a steeper desorption branch. In all the cases described above, adsorption branches of the argon and nitrogen isotherms were similarly steep but desorption branches had considerably different steepness. This confirms our earlier finding[12] that, in the case of MCM-41, the steepness of desorption branches of isotherms may not necessarily be directly related to the quality of materials, but may result from the proximity of the lower limit of pressures at which hysteresis loops are observed. This conclusion is an example of general observations well-known in the scientific literature.[1] Their implication is that the application of desorption branches of isotherms to calculate pore size distributions (PSDs) may lead to artificial narrowing of peaks on PSDs and to occurrence of peaks at similar pore size values for samples with different pore sizes.[1]

It is also interesting that at pressures following the capillary condensation, the overall shapes of argon adsorption isotherms were similar to those of the corresponding nitrogen adsorption isotherms. Namely, for particular MCM-41 samples, the hysteresis loop resulting from the capillary condensation/evaporation in secondary mesopores were in both cases (i) almost

(31) Kruk, M.; Jaroniec, M.; Sayari, A. *Chem. Mater.* **1999**, *11*, 492.
(32) Kruk, M.; Jaroniec, M.; Sakamoto, Y.; Terasaki, O.; Ryoo, R.; Ko, C. H. *J. Phys. Chem. B*, in press.

absent for (2.8), (3.1), (5.1), (5.5), (6.0), and (6.5) MCM-41, (ii) narrow and located at pressures close to the saturation vapor pressure for (2.0) and (3.6) MCM-41, (iii) wide rectangular with a pronounced increase in adsorption close to the saturation vapor pressure for (3.9) and (4.2) MCM-41, or (iv) wide and approximately triangular for (4.6) MCM-41. Since the shapes of these hysteresis loops are likely to reflect certain features of porous structures of the materials under study, this similarity of adsorption behavior of argon at 87 K and nitrogen at 77 K suggests that similar structural information regarding mesopores can be derived from these two kinds of measurements.

Determination of the Total Pore Volume and BET Specific Surface Area from Argon Adsorption at 87 K. BET specific surface areas and total pore volumes determined on the basis of argon adsorption data measured at 87 K are listed in Table 1. The argon total pore volumes were found to be close to those evaluated from nitrogen adsorption data acquired at 77 K,[11,12,27−29] the latter being on average 5% larger than the former. Since, as will be demonstrated later, similar differences were observed between primary mesopore volumes obtained using these two adsorptives, it is unlikely that the difference in the total pore volume resulted from considerable differences in the range of pore sizes in which capillary condensation took place below the relative pressure used for the single-point V_t calculations (that is, 0.99) for these two different adsorptives. However, the differences in the pore volume estimates might have resulted from overestimation of argon density in pores.

Despite the fact that the corresponding total pore volumes evaluated on the basis of argon and nitrogen data were close to one another, BET specific surface areas differed widely. The BET specific surface area estimates from nitrogen data were on the average 29% higher than those based on argon data at 87 K. This difference most likely resulted primarily from the fact that nitrogen BET calculations performed in a typically used relative pressure range (for instance 0.04−0.2) significantly overestimate the monolayer capacity, as shown from the statistical film thickness measurements for large-pore MCM-41.[12,26] As will be shown later, argon BET calculations performed in the same pressure interval allow for a quite reasonable evaluation of the monolayer capacity and thus the resulting estimations of the specific surface area for silicas are suggested to be much more accurate than results of nitrogen BET analysis in the pressure range considered. However, this does not imply that argon BET analysis is inherently better for silicas, since the results of nitrogen BET calculations are highly dependent on the choice of the pressure interval used for calculations.[33] Thus, the determination of a pressure range suitable for the specific surface area calculations using nitrogen data could readily be achieved, if proper reference surface area data were available. The problems of consistent specific surface area calculation from nitrogen and argon adsorption data require further studies, which are beyond the scope of this work, and we anticipate reporting their results in our forthcoming paper.

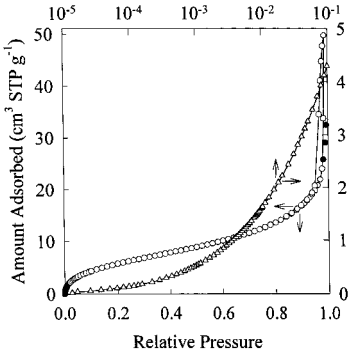

Figure 3. Argon adsorption isotherm measured at 87 K for a LiChrospher Si-1000 macroporous silica (hollow circles for the plot in normal scale and hollow triangles for the plot in logarithmic scale) and its extrapolation for pressures close to the saturation vapor pressure based on an argon adsorption isotherm for a LiChrospher Si-4000 macroporous silica (filled circles).

Reference Argon Adsorption Isotherm and Its Application in the Comparative Analysis. In determination of the primary mesopore volume and external surface area of MCM-41 from argon adsorption data, a suitable reference adsorption isotherm is needed. Therefore, argon adsorption at 87 K was measured on a LiChrospher Si-1000 macroporous silica, which was previously shown to be a suitable reference adsorbent in the case of nitrogen adsorption at 77 K.[27,33] The obtained argon adsorption isotherm is shown in Figure 3. From the point of view of characterization of adsorbents by means of comparative methods, it is beneficial when the adsorption on the reference solid proceeds via monolayer−multilayer adsorption in the entire pressure range. However, LiChrospher Si-1000 exhibited a steep increase in adsorption in the proximity of the saturation vapor pressure and a narrow, yet distinct, hysteresis loop in this pressure region, which indicated capillary condensation in macropores of the sample. To eliminate the influence of this effect, the reference adsorption data for LiChrospher Si-1000 were extrapolated over the relative pressures above 0.97 using an adsorption isotherm for LiChrospher Si-4000, which exhibited a much more gradual increase in adsorption in this pressure range and only a very slight indication of adsorption−desorption hysteresis (see Figure 3). The resulting reference adsorption data for argon adsorption at 87 K on a macroporous silica surface are provided in Table 2.

The reference adsorption isotherm was used to calculate α_s plots for the MCM-41 samples under study. As expected from the previous analysis of nitrogen adsorption data,[12,27−29] the plots exhibited linear segments at α_s values above those corresponding to the capillary condensation in primary mesopores, allowing one to calculate the primary mesopore volumes and the external surface areas for the MCM-41 samples. The obtained structural parameters are listed in Table 3. Similarly to the estimates of the total pore volumes, the primary mesopore volumes determined previously from nitrogen adsorption data at 77 K were close to those determined from argon adsorption data at 87 K (on the

(33) Jaroniec, M.; Kruk, M.; Olivier, J. P. *Langmuir* **1999**, *15*, 5410.
(34) Vargaftik, N. B. *Tables on the thermophysical properties of liquids and gases in normal and dissociated states*; Hemisphere Publishing: Washington, D.C., 1975; p 564.
(35) Barrett, E. P.; Joyner, L. G.; Halenda, P. P. *J. Am. Chem. Soc.* **1951**, *73*, 373.

Table 3. Structural Properties of the MCM-41 Samples under Study Determined from Argon Adsorption Isotherms Measured at 87 K[a]

sample	V_p ($cm^3\ g^{-1}$)	S_{ex} ($m^2\ g^{-1}$)	w_{BJH} (nm)	w_d (nm)	S_{BJH} ($m^2\ g^{-1}$)
(6.5)	0.91	60	6.60	6.53	620[b]
(6.0)	1.02	40	6.05	5.96	740[b]
(5.5)	0.92	40	5.62	5.53	700[b]
(5.1)	0.70	50	5.07	5.11	600[b]
(4.6)	0.49	70	4.60	4.55	480[b]
(4.2)	0.63	120	4.12	4.22	700[b]
(3.9)	0.60	100	3.82	3.88	710[b]
(3.6)	0.70	90	3.49	3.58	880[b]
(3.1)	0.49	50	3.07	3.08	650[b]
(2.8)	0.53	60	2.78	2.76	750[b]
(2.0)	0.20	90	2.28	2.04	480

[a] V_p, primary mesopore volume; S_{ex}, external surface area; w_{BJH}, position of the maximum on the BJH pore size distribution; w_d, primary mesopore size determined on the basis of the XRD interplanar spacing and the primary mesopore volume (the latter calculated from nitrogen adsorption data) using geometrical considerations (eq 1); S_{BJH}, specific surface area evaluated using the BJH method. [b] The BJH specific surface area was calculated for pores wider than 2 nm.

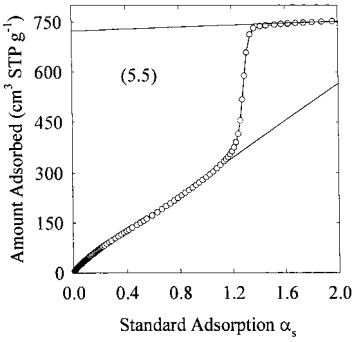

Figure 4. Representative α_s plot for argon adsorption on MCM-41 silica.

average, the former were about 7% higher). The external surface areas evaluated using nitrogen and argon adsorption were also similar.

In contrast to the linear low-pressure parts of α_s plots for MCM-41 calculated on the basis of nitrogen adsorption data at 77 K using reference macroporous silicas (such as LiChrospher Si-1000 used in the current study), low-pressure (low α_s) parts of the α_s plots calculated on the basis of argon data at 87 K were noticeably bent upward (Figure 4). Therefore, formal calculations of the MCM-41 micropore volume from these parts of the plots provided positive values of about 0.02 $cm^3\ g^{-1}$ for all the samples under study, whereas the comparative analysis of nitrogen adsorption data at 77 K usually provides micropore volumes very close to 0.00 (usually $\pm 0.01\ cm^3\ g^{-1}$, rarely outside the range $\pm 0.015\ cm^3\ g^{-1}$). Since argon atom interacts with a solid surface via nonspecific interactions, whereas nitrogen molecule may exhibit specific interactions because of its quadrupole moment,[36] it is not likely that the observed differences in the low-pressure adsorption behavior of argon on MCM-41 and macroporous silica were caused by differences in their surface heterogeneity. Thus, the differences in adsorption behavior were probably caused by structural heterogeneity, that is, by some details of

(36) Rouquerol, J.; Rouquerol, F.; Grillet, Y. *Pure Appl. Chem.* **1989**, *61*, 1933.

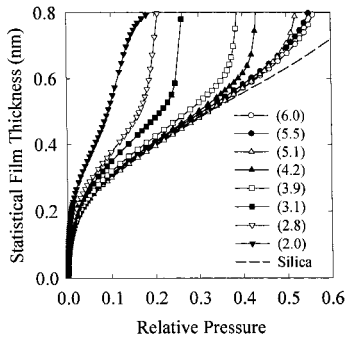

Figure 5. Argon statistical film thickness curves in pores of selected MCM-41 samples and the reference *t*-curve for silicas (data from Table 2).

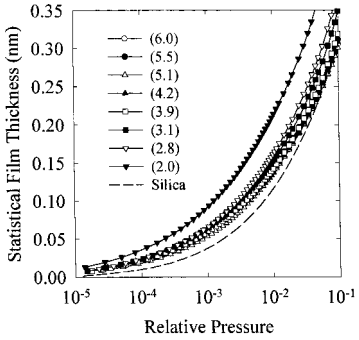

Figure 6. Low-pressure parts of argon statistical film thickness curves in pores of selected MCM-41 samples and their comparison to the low-pressure part of the reference *t*-curve for silicas (data from Table 2).

surface geometry or surface roughness of the materials under study. However, full explanation of the observed behavior will require further studies. Anyway, the observed differences between low-pressure behaviors of MCM-41 and macroporous silica indicate that it may be difficult to quantify relatively small amounts of micropores using comparative plot analysis of argon adsorption data measured at 87 K. If such a determination needs to be carried out, nitrogen at 77 K may provide a much better way to reliably achieve it.

Statistical Film Thickness. Argon statistical film thickness curves (*t*-curves) on the surfaces of MCM-41 pores are shown in Figures 5 and 6. It can be seen that the *t*-curves for sufficiently large pores (those above 5 nm) exhibited a highly similar behavior up to the onset of capillary condensation at relative pressures of about 0.45. Therefore, these *t*-curves were used to establish a reference *t*-curve valid in the entire range of pore sizes. To do this, it was assumed that the reference statistical film thickness at a relative pressure of 0.1 is equal to an average statistical film thickness for (5.1), (5.5), and (6.0) MCM-41 samples. It should be noted that *t*-curve data for the (6.5) MCM-41 were not used since this sample was shown to exhibit detectable microporosity,[27] rendering it unsuitable as a model material for determination of the statistical film thickness.

To facilitate the application of this reference *t*-curve in the pore size analysis, the reference data are provided in Table 2 (multiplication of these data by a proper conversion factor is required). Moreover, their representation by a simple empirical equation (in the form of the Harkins−Jura equation[2]) was found, which is especially accurate in the relative pressure range from

0.1 to 0.95:

$$t(p/p_0)[\mathrm{nm}] = 0.1\left[\frac{10.61}{0.0561 - \log(p/p_0)}\right]^{0.5384} \quad (4)$$

As can be seen in Figure 5, the obtained reference *t*-curve (provided in Table 2) closely followed the data for the large-pore MCM-41 samples up to the relative pressure of about 0.35. At higher pressures, the *t*-curves for MCM-41 samples exhibited gradual upward deviations, which can be attributed to the onset of capillary condensation, as expected from previous studies of nitrogen adsorption in MCM-41 pores.[12] However, the analogy between argon and nitrogen adsorption did not extent over the low-pressure range, as expected from the results of the α_s plot analysis. Namely, nitrogen *t*-curves for MCM-41 samples and adsorption isotherms for macroporous silicas exhibited the same shape at low pressures, allowing for fitting of these curves in the low-pressure range.[12] In contrast, argon *t*-curves for MCM-41 and adsorption isotherms for macroporous silicas measured at 87 K had somewhat different shape at low pressures (see Figure 6). Therefore, it is expected that application of MCM-41 samples in determining the statistical film thickness on silica surfaces is more reliable in the case of nitrogen at 77 K than in the case of argon at 87 K. Anyway, it will be demonstrated later that thus determined *t*-curve for argon at 87 K can be used in calculations of pore size distributions, providing results which are not only self-consistent but also in excellent agreement with those from nitrogen adsorption and combined XRD/adsorption analysis. It also needs to be noted that the derived reference *t*-curve should be considered as an effective *t*-curve for cylindrical pore geometry. If the pores of MCM-41 are hexagonal rather than circular,[32] the actual statistical film thickness in MCM-41 pores would be about 5% lower. Consequently, the reference statistical film thickness (Table 2 and eq 4) would have to be multiplied by the factor of about 0.95 to reflect the actual statistical film thickness. Moreover, despite the fact that large-pore MCM-41 samples were used to determine the reference *t*-curve, it cannot be precluded that the statistical film thickness in these relatively wide pores is still slightly larger than that for a flat surface.

As observed in the case of nitrogen adsorption at 77 K,[12,28,32] the argon *t*-curves for narrower pores exhibited gradual departures from the *t*-curves for the large-pore MCM-41 materials. The differences became more pronounced as the pore diameter decreased (see Figure 5). For samples with pore sizes larger than about 3.5 nm, differences in *t*-curves at low pressures were rather minor (Figure 6), but samples with smaller pore sizes exhibited markedly larger statistical film thicknesses in the low-pressure range.

For the MCM-41 samples other than (2.0) and (2.8), the statistical film thickness at relative pressures where the BET monolayer capacity was reached (that is, 0.12−0.15) was between 0.34 and 0.385 nm, which is similar to the expected statistical monolayer film thickness for argon. The latter can be assumed to be close to the corresponding σ_{ff} Lenard-Jones parameter, which is usually[19,21−24] set to be about 0.34 nm. Thus, argon BET calculations in the relative pressure intervals used in the current study allow for a quite accurate (within about 10%) evaluation of the monolayer capacity for MCM-41 samples with pores larger than 3 nm. This is in contrast to nitrogen BET calculations in the similar relative pressure intervals, which were shown to grossly overestimate the monolayer capacity of MCM-41.[12]

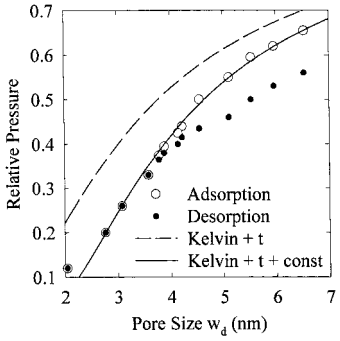

Figure 7. Relations between the capillary condensation/evaporation relative pressures and the pore diameter for cylindrical pores. Hollow and filled circles show experimental capillary condensation (adsorption) and capillary evaporation (desorption) data, respectively. The dashed line represents predictions of the Kelvin equation with the statistical film correction (eq 5). The solid line shows the approximation of the relation between the capillary condensation pressure and the pore size using an interpolation and extrapolation formula based on the Kelvin equation with the correction for the statistical film thickness and an appropriate empirical correction term (eq 6).

Relations between the Capillary Condensation/Evaporation Pressure and the Pore Diameter. Listed in Table 1 and shown in Figure 7 are experimental values of capillary condensation and evaporation pressures (that is, relative pressure values corresponding to midpoints of the capillary condensation/evaporation steps) as functions of the pore diameter determined from XRD/pore volume data using eq 1. As already reported for nitrogen at 77 K,[12] capillary condensation pressure gradually and systematically increased as the pore size increased. In contrast, capillary evaporation pressure exhibited a relatively much smaller increase in the pore size range from about 4 to 5.5 nm, that is, for MCM-41 samples, for which gradual development of hysteresis loops on the adsorption−desorption isotherms was observed (see Figures 1 and 2). This behavior of the desorption data, combined with the lack of a clear relationship between the steepness of desorption branches of the isotherms and the degree of structural ordering, and with the influence of lower limit of the hysteresis behavior on the position of the desorption branches, renders the application of desorption data in mesopore analysis highly inconvenient or even questionable. In contrast, adsorption branches of isotherms appear to be suitable for application in the mesopore size analysis. For such purposes, it is convenient to find an equation, which would adequately describe the relation between the capillary condensation pressure and the pore diameter. Furthermore, it is desirable to have a relation which would exhibit a proper behavior in the limit of large pore sizes, that is, which would be approximately equivalent to the Kelvin equation[1] for sufficiently large pores. As in our previous study of nitrogen adsorption at 77 K,[12] the experimental data for capillary condensation pressure as a function of the pore diameter were initially compared to the Kelvin

equation with the correction for the statistical film thickness:

$$r(p/p_0)[\text{nm}] = \frac{2\gamma V_L}{RT\ln(p_0/p)} + t(p/p_0) = \frac{0.3756}{\log(p_0/p)} + t(p/p_0) \quad (5)$$

where $r(p/p_0)$ is a pore radius as a function of the relative pressure of capillary condensation, R is the universal gas constant (8.314 J mol^{-1} K^{-1}), T is the absolute temperature (about 87.29 K in the case of argon boiling temperature), V_L is the molar volume of liquid argon (28.53 × 10^{-6} m^3 mol^{-1})[1] and γ is the surface tension of liquid argon at argon boiling temperature. The surface tension values reported in the literature vary widely (compare data in refs 1, 19, and 34). In our study, γ was assumed to be equal to 11.00 × 10^{-3} N m^{-1}.[34] The comparison of the predictions based on the Kelvin equation with our experimental data for MCM-41 samples is shown in Figure 7. It can be seen that, even with the correction for the statistical film thickness, the Kelvin equation significantly underestimates the pore size of MCM-41. Since the differences between the experimental data and predictions based on the Kelvin equation were approximately constant in the case of all MCM-41 samples, it was attempted to find a simple empirical correction to this equation in order to improve the agreement with our model data. This approach has already allowed for a successful calibration of pore size distribution calculations from nitrogen adsorption data.[12]

To find a correction term, which would provide a quantitative agreement between the Kelvin equation and the experimental data (see Tables 1 and 3), the latter were fitted with the Kelvin equation with the statistical film thickness correction (eq 5) and with an additional constant correction term.[12] As can be seen in Figure 7, the obtained fit was remarkably good. The obtained expression had the following form:

$$r(p/p_0)[\text{nm}] = \frac{0.3756}{\log(p_0/p)} + t(p/p_0) + 0.438 \quad (6)$$

Calculation of Mesopore Size Distributions from Argon Adsorption Data at 87 K. To test the applicability of eq 6 and the derived statistical film thickness curve (Table 2 or eq 4) for calculation of mesopore size distributions, the Barrett−Joyner−Halenda (BJH) procedure[35] was employed. As can be seen in Table 3, the obtained pore diameter estimations were in a remarkably good agreement (usually better than 0.1 nm) with the pore diameters evaluated on the basis of geometrical considerations (eq 1). Specific surface areas evaluated using the BJH procedure with eq 6 were also found to be close to those from the argon BET calculations (Table 1) as well as to those evaluated using the KJS-calibrated BJH procedure from nitrogen adsorption data at 77 K.[12] In addition, cumulative pore volumes determined using the BJH method were in excellent agreement with the total pore volumes evaluated from the single-point calculations. What is even more remarkable, the peaks on the resulting mesopore size distributions exhibited position, overall shape, width, and height highly similar to those obtained from the KJS-calibrated BJH calculations using nitrogen adsorption data measured at 77 K[12] (see Figure 8). PSDs in the secondary mesopore range were also found to be similar for both of the adsorbates used. It should be noted that, from their very nature, the approach for PSD calculations presented herein is based on an assumption of applicability of a common *t*-curve to describe adsorption on the surface of pores of different sizes. As can be seen in Figures 5 and 6, this assumption becomes increasingly inaccurate as the pore size decreases. The observed differences between the statistical film thickness in MCM-41 pores and the reference *t*-curve are expected to lead to appearance of artificial tails on PSDs. This effect appears to be rather minor for pores above 3 nm in diameter, but PSDs for the samples with narrower pores exhibited more pronounced tails, which extended down to the pore size of about 1 nm (see Figure 8). This behavior was particularly pronounced for (2.0) MCM-41. Thus, because of its underlying assumptions, the KJS-calibrated BJH procedure is suitable primarily for calculation of PSDs for pores above about 2 nm in diameter (that is, in the mesopore range and probably at the lower end of the macropore range) but is not recommended for calculation of micropore size distribution. It is also important to note that the relation between the pore size and the capillary condensation (or secondary micropore filling[1]) pressure was not determined herein for pores below 2 nm, which may lead to additional inaccuracy in calculations in the micropore range.

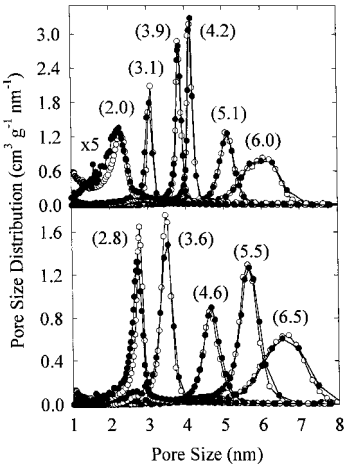

Figure 8. Comparison of mesopore size distributions calculated for MCM-41 samples under study from argon adsorption isotherms at 87 K (hollow circles) and nitrogen adsorption isotherms at 77 K (filled circles) using the BJH calculation procedure with KJS-calibrated *t*-curves and relations between the capillary condensation pressure and pore diameter.

The PSDs evaluated from nitrogen and argon data for samples with pores above about 3.8 nm were essentially the same, whereas, for samples with smaller pore sizes, nitrogen PSDs were somewhat broader (see Figure 8). One can envision the following hypothetical explanation of this finding. It is known from computer simulations and density functional theory calculations that when capillary condensation/evaporation is accompanied with hysteresis, the isotherms for ideal pores of a strictly defined size exhibit vertical capillary condensation steps.[37,38] However, when there is no

hysteresis,adsorption isotherms for such ideal pores have finite slopes.[38] If this is the case for adsorption in real porous systems, calculations of pore size distributions using an assumption about instantaneous and complete capillary condensation at the corresponding capillary condensation pressure are fully valid in the pressure range where hysteresis is observed, but their accuracy at lower pressures depends on the actual slope of the isotherms for ideal pores. The calculation method used in the current study, that is the BJH approach, assumes the existence of a vertical step on adsorption isotherm in the capillary condensation point. Therefore, if the BJH calculation procedure is properly calibrated, it should be possible to obtain highly similar PSDs in the pore size range corresponding to the hysteresis region for both nitrogen at 77 K and argon at 87 K. As discussed above, highly similar PSDs were actually obtained in this case. However, the results of the BJH calculations may differ for lower pore sizes, where adsorption isotherms exhibited no hysteresis. Such differences were actually observed mainly in cases where there was no hysteresis on both argon and nitrogen isotherms and pore diameter was below 3.5 nm. The reasoning presented above further implies that since pore size distributions derived from argon data are narrower, the hypothetical broadening of capillary condensation steps in the region of adsorption/desorption reversibility should be more pronounced in the case of nitrogen at 77 K than in the case of argon at 87 K. Other reasons of the differences in the PSDs obtained from nitrogen and argon data may also be envisioned. For instance, from its very nature, argon adsorption is expected to be less sensitive to the effects of surface heterogeneity than nitrogen adsorption.[36] The effects of surface heterogeneity may lead to broadening of capillary condensation steps[38] and, consequently, the derived PSD peaks. Thus, such broadening should be more pronounced in the case of nitrogen adsorption. Moreover, statistical film thickness in MCM-41 pores is much larger at given relative pressure in the case of nitrogen at 77 K (compare data from the current work and ref 12). Since the capillary condensation relative pressures for pores of a particular size are similar in both cases, the pore core diameter (that of empty space confined by the adsorbate film on the pore walls) at the onset of the capillary condensation is lower in the case of nitrogen at 77 K. Therefore, the effects of fluctuations in the film thickness and in the pore diameter may have a more pronounced influence in the latter case, which in turn may lead to a more significant broadening of the capillary condensation steps and the derived PSDs. The fact that argon PSDs for MCM-41 with small pores are narrower than nitrogen PSDs and its possible explanations discussed above suggest that argon may be better for calculation of pore size distributions for materials with pores at the borderline between the micropore and mesopore range. However, as already discussed, the methodology for PSD determination used in the current study is not fully applicable for such narrow pores.

As discussed above, highly similar mesopore size distributions can be determined from adsorption branches of isotherms for argon at 87 K and nitrogen at 77 K. This is in contrast with results obtained from desorption branches of nitrogen and argon isotherms, which were found to be inconsistent as far as peak position, width, and height as well as the number of peaks are concerned, even though an advanced DFT method of modeling of adsorption in porous media was employed.[21−24] Thus, one can conclude that the KJS approach for testing and improving methods of mesopore size analysis can successfully be applied for different adsorptives, allowing one to achieve excellent agreement between PSD calculations based on data for different adsorptives.

Conclusions

Application of model MCM-41 adsorbents allowed us to determine the reference statistical film thickness curve for silicas and the accurate empirical relation between the capillary condensation pressure and the diameter of cylindrical pores for argon adsorption at 87 K. These relations can readily be used in standard methods to calculate mesopore size distributions, providing results which are in excellent agreement not only with results of properly calibrated nitrogen adsorption analysis but also with pore sizes evaluated independently on the basis of the XRD interplanar spacing and pore volume data. Thus, argon adsorption at 87 K was found be as useful in the mesopore size analysis as nitrogen adsorption at 77 K. There were also some indications that argon adsorption at 87 K may be highly useful in analysis of materials with pore sizes on the borderline between the micropore and mesopore ranges.

Acknowledgment. The donors of the Petroleum Research Fund administrated by the American Chemical Society are gratefully acknowledged for support of this research. Drs. A. Sayari (U. Laval, Canada) and R. Ryoo (KAIST, Korea) are acknowledged for providing MCM-41 samples, which were previously reported in refs 11, 12, and 27−29. The authors also want to thank Dr. J. P. Olivier (Micromeritics, USA) for a helpful discussion and for providing his argon adsorption data for comparison.

CM9905601

(37) Maddox, M. W.; Olivier, J. P.; Gubbins, K. E. *Langmuir* **1997**, *13*, 1737.

(38) Karykowski, K.; Rzysko, W.; Patrykiejew, A.; Sokolowski, S. *Thin Solid Films* **1994**, *249*, 236.